Desalination and Water Treatment
www.deswater.com

doi: 10.1080/19443994.2014.968876

56 (2015) 3294–3304
December

Taylor & Francis
Taylor & Francis Group

Enhancement of productivity of humidification–dehumidification desalination using modified air heater

C. Muthusamy[b], M. Gowtham[a], S. Manickam[a], M. Manjunathan[a], K. Srithar[a,*]

[a]*Department of Mechanical Engineering, Thiagarajar College of Engineering, Madurai 625015, Tamilnadu, India, Tel. +91 9842185302; Fax: +91 4522483427; email: ponsathya@hotmail.com (K. Srithar)*
[b]*Department of Mechanical Engineering, Sethu Institute of Technology, Virudhunagar 626115, Tamilnadu, India, Tel. +91 9942354525; email: samymuthu.c@gmail.com (C. Muthusamy)*

Received 6 December 2013; Accepted 14 September 2014

ABSTRACT

Experimental investigation on humidification–dehumidification (HD) desalination system is carried out with half-perforated circular inserts incorporated in the air heater. These half-perforated circular inserts are provided with the orientation angle of 45, 90, and 180° with two pitches, 114 and 152 mm. Experiments are conducted in the HD desalination unit for various combinations of parameters in the air heater. The productivity of the HD desalination system is based on the mass flow rate, temperature of air and saline water, and also the pitch ratio and orientation angle of the circular inserts. Maximum productivity of 0.82 kg/h is obtained for the orientation angle of 180°, pitch ratio (pitch length/diameter of the pipe) of 3 and the air flow rate of 21 kg/h. The economic analysis is also carried out and the payback period of such a system is found as 171 d.

Keywords: Desalination; Humidification–dehumidification desalination; Air heater; Heat transfer enhancement; Friction factor; Perforated inserts

1. Introduction

Multieffect, multistage flash, reverse osmosis, vapour compression and electro dialysis desalination systems need high capital cost, and the maintenance cost is also very expensive. So, these systems are unaffordable for most of the developing countries. Humidification–dehumidification (HD) desalination systems provide better output with less running cost. In order to enhance the performance of the HD desalination system, various research works had been carried out.

Ghazi-Al Enezi et al. [1] analysed the effect of operating parameters in productivity of the HD desalination system which consists of plain electrical air heater. Summers et al. [2] produced consistent air outlet temperatures throughout the day and night in the air heater of the HD desalination system using the phase-change material storage. Yamali et al. [3] proved that the HD desalination system with double-pass solar air heater showed the increased productivity of 8% when compared with single-pass air heater. Xiong et al. [4] claimed that the heat transfer process in the shell and tube desalting column could be greatly enhanced by baffle plates. Liebenberg and Meyer [5] concluded that the heat transfer can be substantially increased by providing a micro fin tube or helical wire inserts. Bilen et al. [6] experimentally studied the heat transfer rate and the friction factor in the flow of rectangular cross-sectional channel by

*Corresponding author.

using the cylindrical fins. Tijing et al. [7] analysed the effects of star-shaped fin inserts on the heat transfer and pressure drop in a concentric tube heat exchanger provided with various configurations and found that the straight-fin configuration gave good performance. Eimsa-ard et al. [8] investigated the performance of a double-pipe heat exchanger fitted with regularly spaced twisted-tape elements and proved that the heat transfer coefficient increases with the increase in twist ratio and friction factor. Tanda [9] studied the heat transfer enhancement from a hot flat plate with rectangular blocks at different orientation angles, and observed that the heat transfer enhancement depends on the space between the blocks and the orientation angle. Ko and Anand [10] experimentally studied the average heat transfer coefficients of a uniformly heated rectangular channel with wall-mounted porous baffles. The use of the porous baffles increased the heat transfer as high as 300% compared to the straight channel without baffles. Suresh et al. [11] experimentally studied the heat transfer and friction factor characteristics of CuO/water nanofluid under turbulent flow in a helically dimpled tube.

Most of the previous works dealt with the improvement of heat transfer rate in the air heater using various inserts without discussing the effect of enhancement of heat transfer rate in the overall productivity of the HD desalination system. Also, it has been noted from the previous work that the productivity enhancement depends on higher air and water temperature in the humidifier. The objective of this research is to augment the productivity of the HD desalination system by means of developing flow turbulence in the passage of air heater using the circular inserts with perforations on half-side. Experiments are carried out with two pitch ratios and three different orientations of the half-perforated circular inserts, and also by varying the mass flow rate of the process air.

2. Mathematical model

The mathematical model for the HD–desalination process includes energy and material balances for all the components of the system.

Following assumptions are considered in the model analysis.

(1) Steady-state operation is assumed.
(2) No heat loss takes place in the humidifier as the wall is fabricated by PVC.
(3) Air leaves the humidifier at saturated condition.

As is shown, during humidification, water evaporates from the water stream into air. This is also associated with the removal of latent heat for evaporation from the water stream as well as the transfer of sensible heat from the water to the air stream. During the dehumidification process, the heat and mass transfer processes are reversed, where water condenses from the air stream. Also, latent and sensible heat is transferred from the air stream to the cooling water stream.

Applying energy balance at the air heater, the heat generated in the air heater was found to be equal to the sum of the heat transferred to the air and the losses.

$$Q_{\text{gen}} = Q_{\text{a}} + \text{Losses} \tag{1}$$

The losses are due to convection and radiation from the air heater to the surrounding. The air flows through the circular tube with uniform heat flux conditions. At the steady state, the heat absorbed by the air is assumed to be equal to the convective heat transferred from the test section. Considering negligible heat losses due to perfect insulation, for finding out the internal convective heat transfer coefficient, only the sensible heat absorbed by the air is considered. No phase change occurred during the process of heating [8], then

$$Q_{\text{a}} = Q_{\text{con}} \tag{2}$$

Heat absorbed by the air from the electrical air heater is given as

$$Q_{\text{a}} = m_{\text{a}} C_{P,\text{a}} (T_2 - T_1) \tag{3}$$

Heat transferred to the air by the convection as given as

$$Q_{\text{con}} = hA(T_s - T_b) \tag{4}$$

By equating the above two equations, the heat transfer coefficient can be found out

$$m_a C_{P,a} (T_{a2} - T_{a1}) = hA(T_s - T_b) \tag{5}$$

The energy balance in the water heater is given above.

The energy available at the inlet of the water heater is,

$$Q = \text{Energy from the heater electrical } (VI) + \text{Energy from recycling from tank 3 and 4} \tag{6}$$

The energy available at the output of the water heater is as follows:

Heat absorbed by the water from the electrical heater is (Fig. 1).

$$Q_{\mathrm{w}} = m_{\mathrm{w}} C_{\mathrm{P,w}} (T_4 - T_3) \tag{7}$$

Heat transferred to the water by the convection is

$$Q_{\mathrm{w}} = hA(T_{\mathrm{s}} - T_{\mathrm{b}}) \tag{8}$$

Energy available in the saline water collected in tank 3 is

$$Q = m_{\mathrm{w9}} C_{\mathrm{p,w}} (T_9 - T_{\mathrm{atm}}) \tag{9}$$

Available energy in the tank 4 is

$$Q = m_{cw} C_{\mathrm{p,w}} (T_6 - T_{\mathrm{atm}}) \tag{10}$$

Available energy in the tank 2 is

$$Q_i = m_{\mathrm{w9}} C_{\mathrm{p,w}} (T_{\mathrm{w9}} - T_{\mathrm{atm}}) + m_{\mathrm{cw}} C_{\mathrm{p,w}} (T_{\mathrm{w6}} - T_{\mathrm{atm}}) \tag{11}$$

The condenser heat transfer area A_C can be calculated by the following equation

$$m_{\mathrm{cw}} C_{\mathrm{p,w}} (T_6 - T_5) = U_{\mathrm{c}} A_{\mathrm{c}} \mathrm{LMTD_c} \tag{12}$$

$$\mathrm{LMTD_c} = \frac{[(T_7 - T_6) - (T_8 - T_5)]}{\ln\left(\frac{T_7 - T_6}{T_8 - T_5}\right)} \tag{13}$$

The humidifier energy balance is given below as,

$$m_{\mathrm{w}} C_{\mathrm{p,w}} (T_4 - T_9) = m_a (H_7 - H_2) \tag{14}$$

Condenser energy balance is

$$m_{\mathrm{cw}} C_{\mathrm{P,w}} (T_6 - T_5) = m_{\mathrm{a}} (H_7 - H_8) \tag{15}$$

The overall mass transfer coefficient is

$$\left(\frac{m_{\mathrm{a}}}{m_{\mathrm{w}}}\right)(H_7 - H_2) = m_D \left[\frac{(H_4 - H_7) - (H_9 - H_2)}{\ln\dfrac{(H_4 - H_7)}{(H_9 - H_2)}}\right] \tag{16}$$

The production flow rate is

$$m_{\mathrm{dw}} = m_{\mathrm{a}} (W_7 - W_8) \tag{17}$$

The water vapour pressure at the dry-bulb temperature is

$$P_{\mathrm{d}} = \varphi P_{\mathrm{s}} \tag{18}$$

Absolute humidity of air is given in the following relation as

$$W = 0.62198 \frac{P_{\mathrm{d}}}{P_{\mathrm{a}} - P_{\mathrm{d}}} \tag{19}$$

The air enthalpy is given by

$$H_a = \left(C_{\mathrm{pa}} + 1.88\right) T_{\mathrm{a}} + W_{\mathrm{a}} \lambda \tag{20}$$

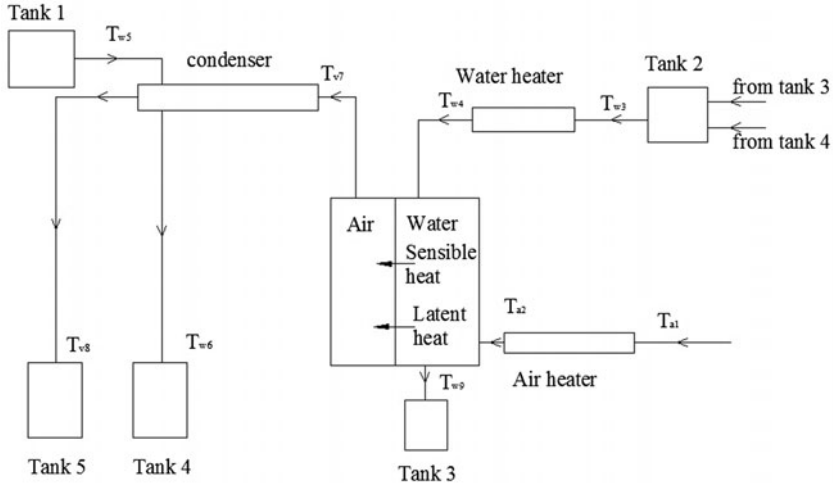

Fig. 1. Mathematical modeling of the system.

The water specific heat at constant pressure is given by

$$C_p = \left(4206.8 - 1.1262T + 1.2026 \times 10^{-2}T^2 + 6.877 \times 10^{-7}T^3\right) \times 10^{-3} \quad (21)$$

The latent heat for water evaporation is given by

$$\lambda = 2501.89 - 2.4070T + 1.1922 \times 10^{-3}T^2 - 1.5863 \times 10^{-5}T^3 \quad (22)$$

Eq. (5) is used to calculate the heat transfer coefficient in the air heater. Eq. (12) is used to calculate the overall condenser heat transfer coefficient. Eqs. (14) and (15) give the energy balance in the humidifier and condenser, respectively. Eq. (16) is used to calculate the overall mass transfer coefficient. Eq. (17) is used to calculate the production rate of fresh water.

3. Experimentation

A laboratory-scaled HD desalination system is considered for this study, which mainly consists of air heater, water heater, humidifier chamber and double-pipe condenser unit. Fig. 2(a) shows the schematic diagram of the HD desalination system.

The air heater chamber consists of the pipe of 1,000 mm in length and 38 mm in diameter, and electric band heater of 500 W to supply constant heat. In order to enhance heat transfer rate in air heater of the HD desalination system, half-perforated circular inserts are used.

The half-perforated circular plates mounted on a stiff central rod are shown in Fig. 2(b). In each circular plate, 15 holes are drilled on a semi-circular pattern. Two pitch ratios of 3 and 4 with orientation (angle of rotation between successive inserts from the point of reference) of 45°, 90°, and 180° are considered. The various types of baffles used in the present study are represented in Table 1.

The first three digits represent the baffle orientation angles in degrees and the next three digits represent its pitch distances in mm.

The water heater consists of an electrical band heater of 1 KW fitted over a galvanized iron pipe of 13 mm diameter and 500 mm length. The humidifier chamber is made of a plastic cylinder of 152 mm diameter and 800 mm height. This humidifier chamber is provided with well-oriented gunny bags as packing material in order to increase the contact period between the process air and the saline stream. The double-pipe condenser with its condensation zone made up of an aluminium pipe with 32 mm diameter and 1,000 mm length, and the outer tube channel of 63.5 mm diameter and 1,000 mm length. The saline water in tank 3 and tank 4 is recycled to tank 2 to extract the energy available in the exit saline water.

The blower is switched on and the mass flow rate of process air is set by the valve V_1. The process air enters the air heater and gets heated, and the saline

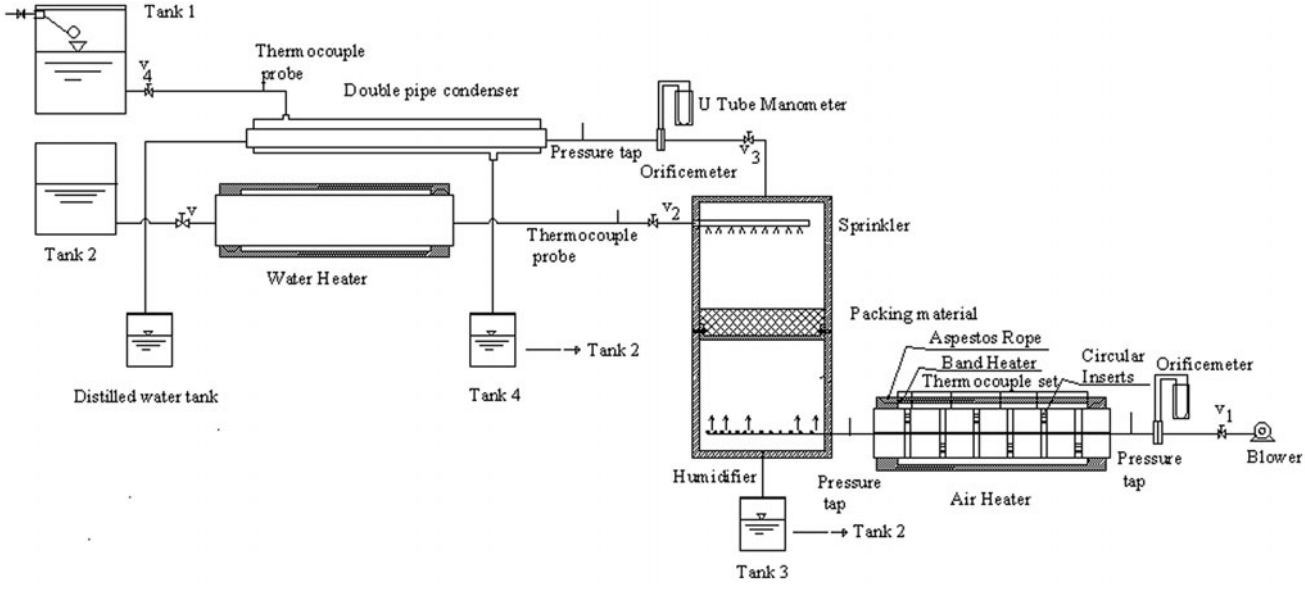

Fig. 2(a). Schematic diagram of experimental system.

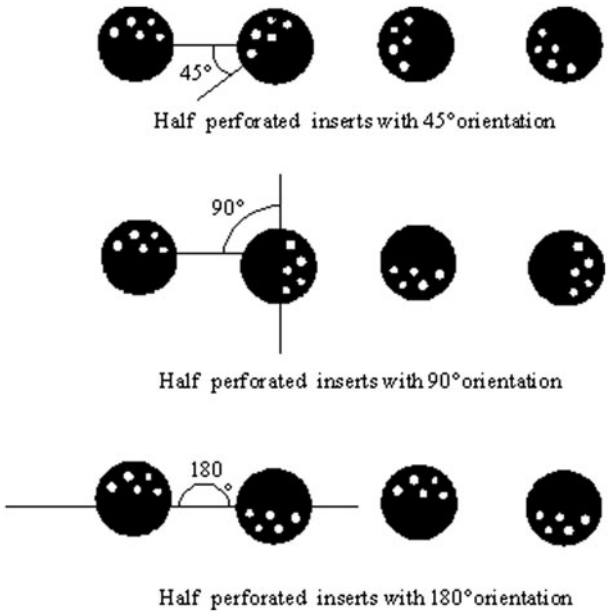

Fig. 2(b). Circular inserts with various orientation

water passing through the water heater is heated by the electrical band heater and sprinkled from the top of the humidifier. The hot process air enters the humidifier and moves upwards, where it becomes humidified due to the heat and mass transfer between the hot saline water and hot air.

The moist air from the humidifier chamber enters the double-pipe condenser for condensation. The saline water in tank 1 flows into the outer tube of the condenser through valve V_4, and absorbs heat from the humid air which is flowing in the inner pipe of the condenser. Counter flow is maintained between the above two fluids to achieve the maximum rate of heat transfer. The condensed water is collected at the distillate tank.

After reaching the steady state, the air temperature at inlet and outlet of air heater, humidifying chamber, condenser and temperature of water at inlet and outlet of water heater, humidifying chamber and condenser are measured. "K" type thermocouples are used to measure the temperatures. The relative humidity at the inlet and outlet of humidifier, mass flow rate of the hot water inlet to the humidifier and the mass flow rate of hot air inlet to the humidifier are also measured. A hygrometer is used to measure the relative humidity and the manometer is used to measure the pressure drop of the air. Orifice meter is used to measure the flow rate of the process air.

Heat transferred to the air by the convection can be determined by [8],

$$Q_{\text{con}} = hA(T_{\text{w}} - T_{\text{b}}) \tag{23}$$

using Eq. (2), the average heat transfer coefficient can be calculated and the fully developed Nusselt number is evaluated using the relation [8],

$$Nu = \frac{hd}{k} \tag{24}$$

The Darcy friction factor can be determined by [8],

$$f = \frac{2d\Delta \text{P}}{\rho l v^2} \tag{25}$$

The thermal performance factor I_E can be used to compare the heat transfer coefficient of the air heater with and without inserts. It is the ratio of the heat transfer coefficient with and without the circular inserts to the friction factor with and without the circular inserts.

$$I_E = \frac{\frac{h_{\text{wt}}}{h_{\text{wot}}}}{\left(\frac{f_{\text{wt}}}{f_{\text{wot}}}\right)^{0.272170}} \tag{26}$$

Experiments were conducted for various combinations of parameters like: the mass flow rate of air, orientation of the half-perforated circular inserts and the pitch ratio of inserts. Mass flow rate of air is varied between 14 and 21 kg/h. The Reynolds number discussed in the graphical analysis of the result analysis is given by [8],

Table 1
Configurations of circular inserts arrangements

Circular insert types	Orientation angle (β) in degrees	Pitch distance (H) in mm	Pitch ratio (PR)
180050	180	50	1.5
180100	180	100	3
090050	90	50	1.5
090100	90	100	3
045050	45	50	1.5
045100	45	100	3

$$\mathrm{Re} = \frac{\rho v d}{\mu} \tag{27}$$

All the thermo-physical properties of air are determined by the overall bulk mean temperature of air.

3.1. Error analysis

Error analysis is carried out for the thermometer, temperature indicator, manometer, voltmeter and ammeter. The minimum error that occurs in any instrument is equal to the ratio of its least count to the minimum value of output measured.

The uncertainties in the measurements are defined [12] as the root sum square of the fixed error of the instrumentation and random error observed at various measurements.

The characteristics of the various measuring instruments used in the experiments are given in Table 2.

Uncertainties associated with the dependent variables like Reynolds number, friction factor and Nusselt number are also estimated using the following equations [11]. Uncertainty in a measurement consists of two major components such as bias error and random error. Bias error is a constant and systematic error in the process. Random error is the repeatability error. The uncertainty in the experimental measurements is defined as the root mean square of the fixed error and the random error.

$$\text{Uncertainity} = \sqrt{(B^2 + R^2)} \tag{28}$$

$$\frac{\Delta \mathrm{Re}}{\mathrm{Re}} = \left[\left(\frac{\Delta m}{m}\right)^2 + \left(\frac{\Delta d}{d}\right)^2\right]^{0.5} \tag{29}$$

$$\frac{\Delta f}{f} = \left[\left(\frac{\Delta(\Delta p)}{\Delta p}\right)^2 + \left(\frac{\Delta l}{l}\right)^2 + \left(3\frac{\Delta d}{d}\right)^2 + \left(2\frac{\Delta \mathrm{Re}}{\mathrm{Re}}\right)\right]^{0.5} \tag{30}$$

$$\frac{\Delta \mathrm{Nu}}{\mathrm{Nu}} = \left[\left(\frac{(\Delta V)}{V}\right)^2 + \left(\frac{\Delta I}{I}\right)^2 + \left(\frac{\Delta d}{d}\right)^2 + \left(\frac{\Delta T_s}{T_s}\right)^2 + \left(\frac{\Delta T_b}{T_b}\right)^2\right]^{0.5} \tag{31}$$

The calculations pointed out that the uncertainties involved are ±0.5% for Reynolds number, ±1.4% for friction factor and ±0.14% for Nusselt number. The experimental results are reproducible within these uncertainty ranges.

4. Results and discussion

The effect of half-perforated circular inserts equipped in the air heater on the performance of all the components of the HD desalination system at different stages is discussed here.

4.1. Performance analysis of air heater

Half-perforated circular inserts with various angles of orientations are used to make the turbulent motion of air in the air heater which leads to enhance the heat transfer.

4.1.1. Variation of Nusselt number with Reynolds number

Fig. 3 shows the comparison of Nusselt number and Reynolds number for the inserts with pitch ratios of 3 and 4. The Nusselt number quantifies the amount of heat transfer taking place in the air heater unit. The orientation angles between successive plates in the half-perforated circular inserts as 45˚, 90˚, and 180˚, and two pitch ratios of 3 and 4 are considered for analysis. It is identified that the heat transfer coefficient of air in an air heater with the circular inserts is directly proportional to Reynolds number and the angle of orientation, and inversely proportional to pitch ratio.

Table 2
Accuracies and ranges of measuring instruments

Instrument	Range	Accuracy	Uncertainty (%)
Temperature indicator	0–500˚C	±1˚C	3.3
Manometer	500 mm	1 mm	4
Orifice meter	500 mm	1 mm	4
Ammeter	0–20 amp	0.01 amp	0.2
Voltmeter	0–220 V	0.1 V	0.2
Hygrometer	0–100	±1	1

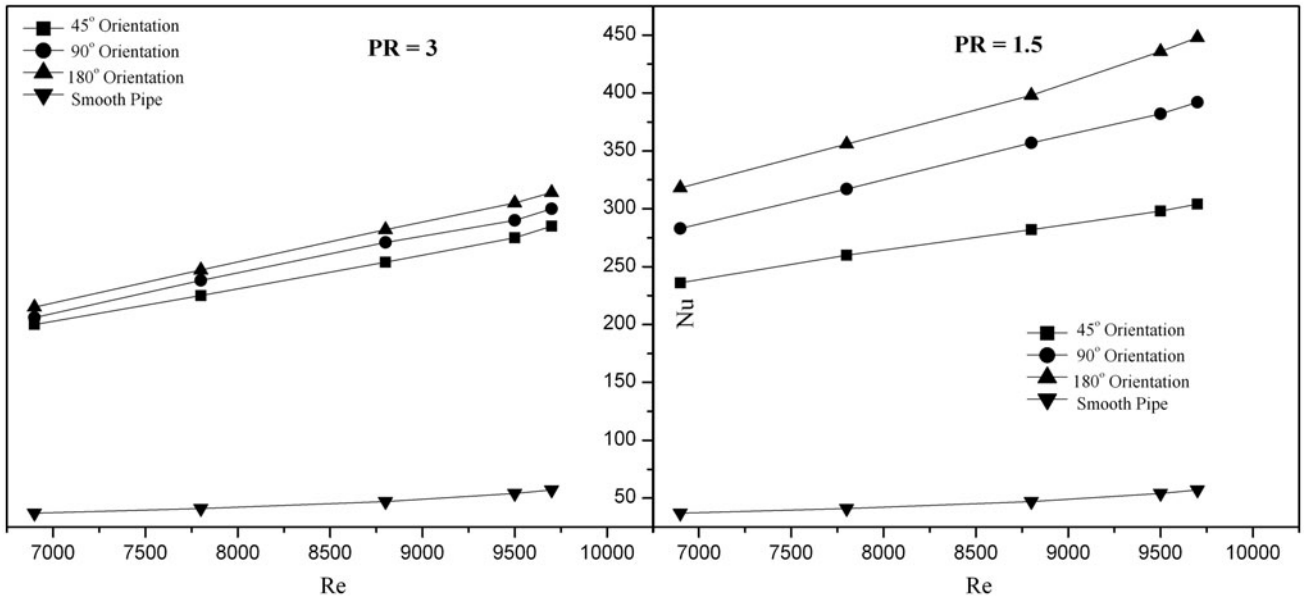

Fig. 3. Nusselt number with Reynolds number.

As the pitch ratio decreases from 4 to 3 the pressure drop increases which increase the residence time of air in the air heater. Higher orientation angle creates more turbulence effect on air resulting in the higher air outlet temperature. From the experiment, the maximum heat transfer rate is shown for Reynolds number of 9,800 with a pitch ratio of 3 and the orientation angle of 180˚. The maximum order of the enhancement of the circular inserts was found nine times of the plain tube.

4.1.2. Effect of Reynolds number on friction factor

It is customary to express the pressure drop in flow through pipe is related to the friction factor. Experiments on the air heater proved that the friction factor increases with increase in orientation angle and the decrease in pitch ratio of the inserts, and decreases with increase in Reynolds number. It can be seen from Fig. 4, the friction factor is higher for pitch ratio of 3. Because short pitch ratio increases the pressure drop which also leads to increase in friction factor. The maximum friction factor in the air heater is obtained for the pitch ratio of 3, orientation angle of 180˚ and the lowest Reynolds number of 6,800.

4.1.3. Comparison of thermal performance factor and friction loss

Fig. 5 shows the variation of thermal performance factor I_E in the air heater with Reynolds number for the different orientation of baffle inserts $\beta = 45^\circ$, 90˚ and 180˚ with PR = 3 and 4. The thermal performance factor relates the ratio of the heat transfer coefficient to the ratio of friction factor compared to the plain tube.

The half-perforated baffles of 180˚ orientation gives the highest thermal performance at all Reynolds numbers and gives the maximum of 4.8 for PR = 3 and 3.4 for PR = 4. The perforated baffles of 45˚ orientation give the lowest thermal performance factor at all Reynolds numbers. In addition, the thermal performance factor increases as the pitch ratio decreases.

4.2. Performance analysis of humidifier

The humidifier performance greatly depends on the inlet mass flow rates and the temperature of water and air. Observations are made about the humidifier based on various orientations, pitch ratios of the inserts in air heater and also mass flow rate of the air in the air heater.

4.2.1. Effect of air temperature on relative humidity

Fig. 6 shows the effect of air temperature on the relative humidity. At constant mass flow rate of air, the increase in air temperature leads to increase the productivity. As explained in Section 4.1.1, with the aid of half-perforated circular inserts in the air heater, the increase of residence time and the turbulent motion created in the air heater simultaneously increases the air outlet temperature. At higher air temperature, the decrease of relative humidity leads to

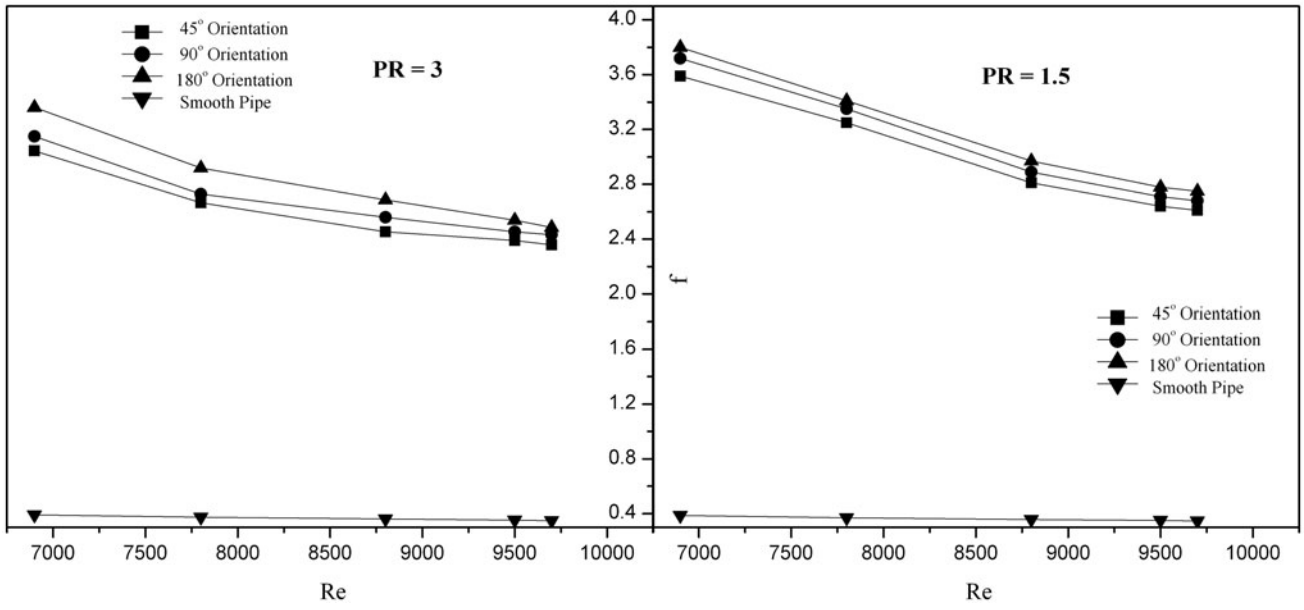

Fig. 4. Friction factor with Reynolds number.

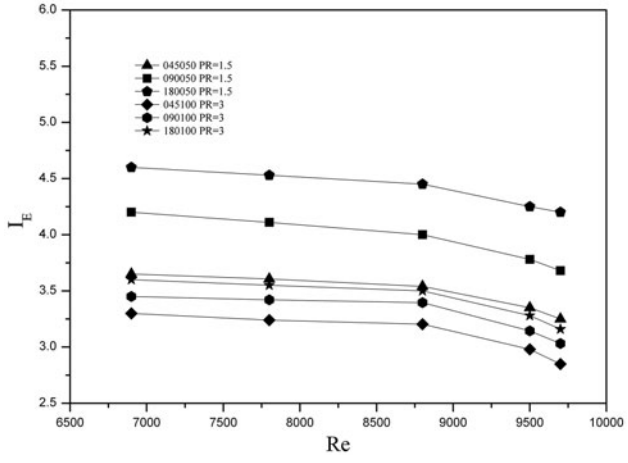

Fig. 5. Variation of Reynolds number and thermal performance factor.

increase the capability of air to absorb the water vapour from the feed water and simultaneously increases the output distillate flow rate. The maximum relative humidity of 90% was attained for pitch ratio of 3 and orientation angle of 180˚. The increase of humidity ratio increases the productivity.

4.2.2. Effect of water temperature on productivity

Fig. 7 expresses the relation between the mass of distilled water production and the mass of air for various hot water temperatures in the humidifier for the constant mass flow rate of water. The air temperature is escalated to enhance the ability to hold water vapour by increasing the temperature of water. Thus, the humidity ratio of air leaving the humidifier increases as well as it increases the system productivity. For the constant flow rate of water, the productivity of the unit distillate increases as the water temperature is increased.

4.3. Performance analysis of condenser

Condensation depends on the cooling effect produced by the cooling water circuit. The mass flow rate and the relative humidity of hot and humid air passing through the inner tube of the condenser have an effect over the mass of condensate produced.

The productivity of the HD desalination unit is directly proportional to the outlet humidity of the humidifier. The increase of air temperature due to the integration of half-perforated circular insert in the air heater increases the moisture absorption in the humidifier which leads to increase the extraction of distilled water in the condenser.

In Fig. 8, the effect of the mass flow rate of air on the productivity is shown for the PR = 3 and 4 of inserts in the air heater. It is seen from the plot that the mass flow rate of air is directly proportional to the mass of condensate obtained. This is due to the increase of mass transfer coefficient, and it also increases the possibility of mixing water in the humidification chamber which leads the capacity of holding

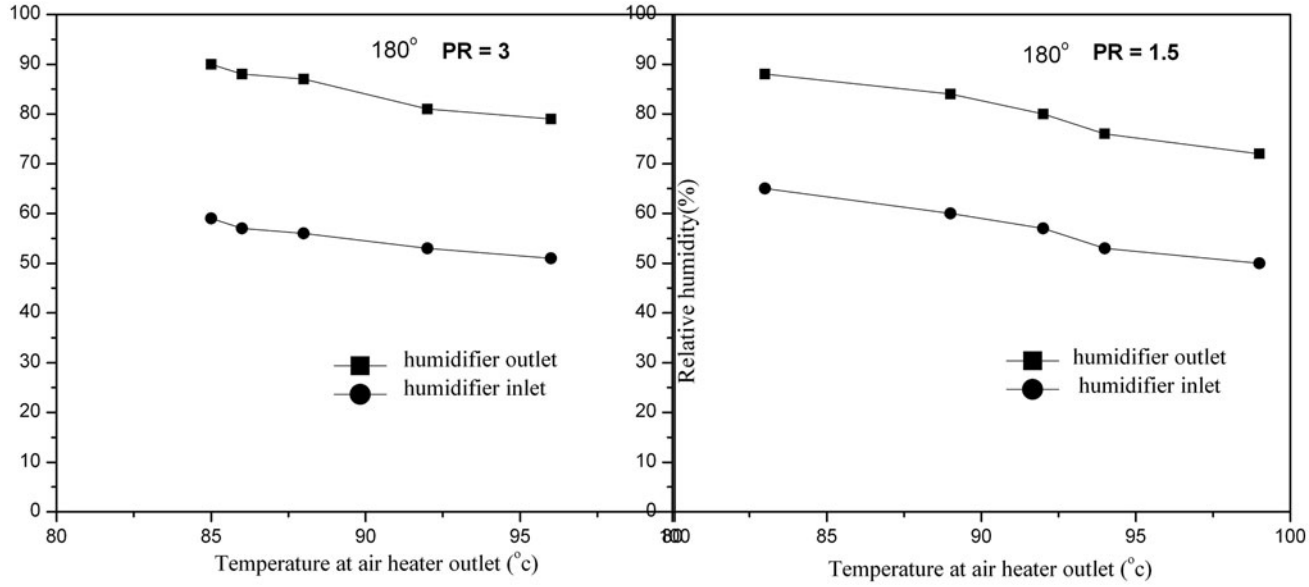

Fig. 6. Effect of relative humidity on air temperature.

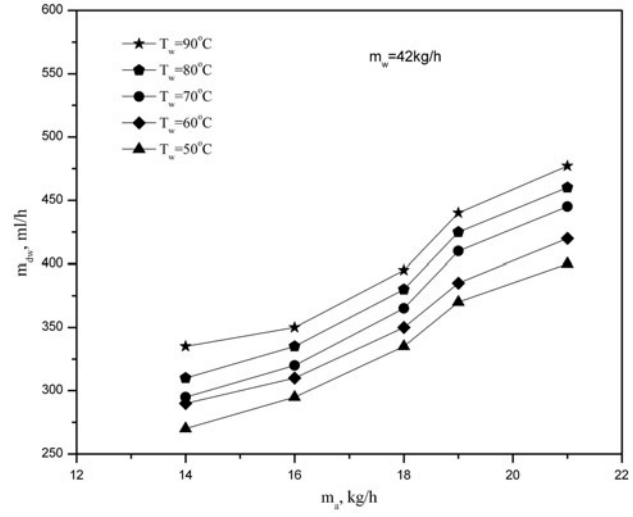

Fig. 7. Effect of water temperature on mass of condensate.

more water vapour at high flow rate. The heat transfer augmented in the air heater with 180° orientation angle with a mass flow rate of air 21 kg/h yields the maximum productivity.

Based on the blower capacity and valve arrangement in this work, the air flow rate is ranged from 14 to 21 kg/h. From the figure, it can be concluded that the increase in mass flow rate of air increases the production of distilled water. The productivity can be increased for further increase in mass flow rate of air.

4.4. Water analysis

The chemical analysis of input salt water and final condensed distilled water is conducted at the research centre of Sethu Institute of Technology, Kariapatti to identify the suitability of the distillate for various purposes. The analysis details are given in Table 3.

4.5. Economic analysis

The important parameters for estimating water production costs are the equipment cost (fixed cost), the operating cost. The total cost is the summation of fixed-charge cost and operating cost. The fixed-charge cost is obtained by multiplying the total direct and indirect cost by amortization factor "a". The operating cost includes all expenditure involved other than equipment cost.

$$a = \left[\frac{[i(1+i)^n]}{(1+i)^n - 1}\right] \tag{32}$$

The payback period of the experimental set-up depends on the overall cost of fabrication, operating cost and maintenance cost. Fabrication cost includes cost of air heater, water heaters, humidification chamber, condenser, blower, valves and stands.

The overall fabrication cost (present experimental setup) = ₹7,500 (136$)

Air heater (500 mm length), water heater (500 mm length) and humidifier (0.75 m)

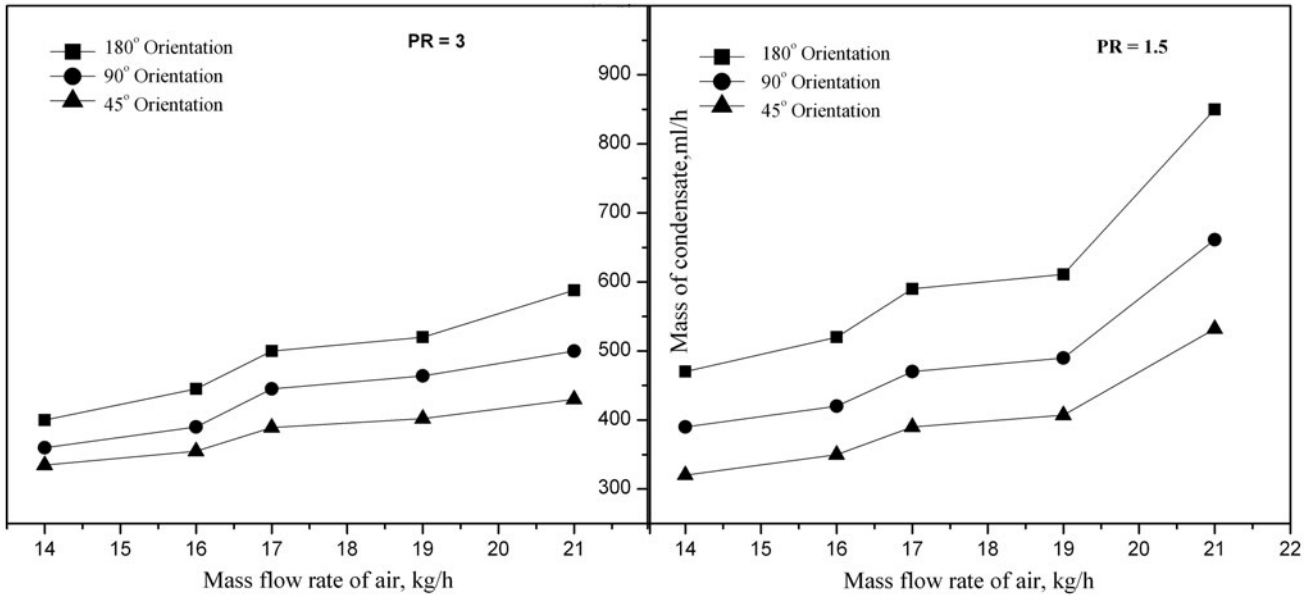

Fig. 8. Variation of mass of condensate with mass flow rate of air.

Table 3
Water analysis

Type of water	PH	Total suspended solids (mg/L)	Hardness (mg/L)	Chloride (mg/L)	Turbidity (NTU)
Salt water	8.2	40	158	32.90	11
Distilled water	7.8	8	147.5	3.19	7
Drinking water (as per IS 10500)	6.5–8.5	100–200	300	250	10

Condenser (1 m length inner pipe and shell, water storage tanks)

Cost per litre of distilled water = ₹10 (0.18$)

Output per hour = 820 ml/h

Daily productivity of the desalination unit (8 h) = 6.56 l

Cost of water produced = ₹65.6(1.25$)

Electrical power used per hour = 1.9 units

Electricity charges = ₹1.5 per unit (0.0271$)

Cost of electricity per hour = ₹2.85 (0.0516$)

Cost of electricity per day (8 h) = ₹22.80 (0.412$)

Cost of mineral per litre = ₹0.20 (0.0036$)

Total cost of mineral per day = ₹1.36 (0.024$)

Net earnings per day = (Cost of water produced—(electricity charges+ cost of minerals)) = (65.6-(22.80 + 1.36)) = ₹41.44 (0.81$)

Payback period = Investment/net earnings = ₹7,500 (136$)/₹41.44 (0.81$) = 171 d

The economic analysis is done by considering overall fabrication cost for the increased scale of unit; the overall running cost increased for the increased mass flow rate is considered by the simultaneous increase of the electric power cost, but it can be justified by the corresponding production of the distilled water.

5. Conclusion

The productivity of the HD desalination system is augmented by the air heater equipped with the half-perforated circular inserts kept with three different orientations and two pitch ratios. It is found that, the heat transfer enhancement in the air heater is 900% higher than the plain tube and also the maximum productivity of distilled water (0.82 kg/h) can be attained at the optimum mass flow rate of air of 21 kg/h for the angle of orientation of the inserts of 180° and pitch ratio 3.

The distillation yield increases with the increase of mass flow rate in water, air and friction factor and the

decrease of pitch ratio of the inserts. Due to the increase in friction factor, the outlet temperature of air in the air heater increases and it simultaneously leads to increase the evaporation rate of water.

Without huge investment, the productivity in the HD desalination system is augmented. The economic analysis is also carried out and the Payback period is also within a year (171 d).

Symbols

a	—	amortization factor
A	—	area, m^2
B	—	bias error
C_p	—	specific heat at constant pressure, J/kg K
d	—	inner diameter of the air heater, m
f	—	friction factor
h	—	heat transfer coefficient, W/m^2 K
H	—	enthalpy, J/kg
i	—	annual interest rate
I	—	current, amps
K	—	thermal conductivity, W/m K
l	—	length of the pipe, m
m	—	mass flow rate, kg/s
m_D	—	mass transfer coefficient, m^2/s
Nu	—	Nusselt number
n	—	plant life
P_d	—	water vapour pressure of air, Pa
P_s	—	saturated water vapour pressure, Pa
P_a	—	atmosphere pressure, Pa
Q	—	heat, W
R	—	random error
Re	—	reynolds number
T	—	temperature, K
U	—	overall heat transfer coefficient, W/m^2 K
v	—	velocity, m/s
V	—	voltage, volts
W	—	specific humidity, kg water/kg dry air

Greek symbols

Φ	—	relative humidity
λ	—	latent heat of vapourization, J/kg K
ρ	—	density, kg/m^3
μ	—	dynamic viscosity, kg $m^{-1}s^{-1}$

Subscripts

1	—	air heater input
2	—	air heater output
3	—	water heater input
4	—	water heater output
5	—	cooling water input
6	—	cooling water output
7	—	vapour input to condenser
8	—	distilled water output from condenser
9	—	saline water output from humidifier
a	—	air
atm	—	ambient
b	—	mean temperature
c	—	condenser
cw	—	cooling water
con	—	convection
dw	—	distilled water
gen	—	generated
s	—	surface
v	—	vapour
w	—	water
wt	—	with turbulator
wot	—	without turbulator

References

[1] G. Al-Enezi, H. Ettouney, N. Fawzy, Low temperature humidification dehumidification desalination process, Energy Convers. Manage. 47 (2006) 470–484.

[2] E.K. Summers, M.A. Antar, J.H. Lienhard, Design and optimization of an air heating solar collector with integrated phase change material energy storage for use in humidification–dehumidification desalination, Sol. Energy 86 (2012) 3417–3429.

[3] C. Yamalı, I. Solmuş, Theoretical investigation of a humidification–dehumidification desalination system configured by a double-pass flat plate solar air heater, Desalination 205 (2007) 163–177.

[4] R. Xiong, S. Wang, Z. Wang, A mathematical model for a thermally coupled humidification–dehumidification desalination process, Desalination 196 (2006) 177–187.

[5] L. Liebenberg, J.P. Meyer, In-tube passive heat transfer enhancement in the process industry, Appl. Therm. Eng. 27 (2007) 2713–2726.

[6] K. Bilen, U. Akyol, S. Yapici, Heat transfer and friction correlations and thermal performance analysis for a finned surface, Energy Convers. Manage. 42 (2001) 1071–1083.

[7] L.D. Tijing, B.C. Pak, B.J. Baek, D.H. Lee, A study on heat transfer enhancement using straight and twisted internal fins, Int. Commun. Heat Mass Transfer 33 (2006) 719–726.

[8] S. Eiamsa-ard, C. Thianpong, P. Promvonge, Experimental investigation of heat transfer and flow friction in a circular tube fitted with regularly spaced twisted tape elements, Int. Commun. Heat Mass Transfer 33 (2006) 1225–1233.

[9] G. Tanda, Heat transfer in rectangular channels with transverse and V-shaped broken ribs, Int. J. Heat Mass Transfer 47 (2004) 229–243.

[10] K.-H. Ko, N.K. Anand, Use of porous baffles to enhance heat transfer in a rectangular channel, Int. J. Heat Mass Transfer 46 (2003) 4191–4199.

[11] S. Suresh, M. Chandrasekar, S. Chandra Sekhar, Experimental studies on heat transfer and friction factor characteristics of CuO/water nanofluid under turbulent flow in a helically dimpled tube, Exp. Therm. Fluid Sci. 35 (2011) 542–549.

[12] N.C. Barford, Experimental Measurements: Precision, Error and Truth, second ed., Wiley, New York, NY, 1990.